High Thermal Conductivity Mesophase Pitch-Derived Graphitic Foams

James Klett

Carbon and Insulation Materials Technology Group, Metals and Ceramics Division,
Oak Ridge National Laboratory, Oak Ridge TN, 37831-6087

1. Introduction

In recent years there has been an increasing number of applications requiring more efficient and lightweight thermal management such as high-density electronics, hybrid diesel-electric vehicles, communication satellites, and advanced aircraft. The primary concerns in these thermal management applications are high thermal conductivity, low weight, low coefficient of thermal expansion, high specific strength and low cost (1). Such applications have focused on sandwich structures (a high thermal conductivity material encapsulating a structural core material) to provide the required mechanical properties (1). However, since structural cores (e.g. honeycombs) are typically low-density materials, the thermal conductivity of the overall composite through the thickness is relatively low (~3-10 W/m·K for aluminum honeycomb) (2, 3). One potential core material being explored is metallic foam: however, the thermal conductivities are still low, 5 - 50 W/m·K (3) and are not significantly greater than the out-of-plane thermal conductivities of typical carbon-carbon composites (see Table 1).

Existing carbon foams are typically reticulated glassy carbon foams with a pentagonal dodecahedron structure (7-9), illustrated in Figure 1, and typically exhibit thermal conductivities less than 1 W/m·K (3, 10 - 12). Other pitch-derived carbon foams have been reported and explored. Unfortunately, these are also thermally insulating and are designed for structural reinforcement rather than thermal management. The pitch-derived graphitic foams reported here

exhibit a spherical morphology, and present a unique solution to this problem by offering high thermal conductivity with a low weight.

In order to produce high stiffness and high thermal conductivity graphitic foams, a mesophase pitch invariably must be used as the precursor, thus assuring a graphitic-like (or turbostratic) structure in the ligaments (13-15). Typical foam forming processes utilize a blowing technique, or pressure release, to produce foam of the pitch precursor (14, 16-19). As the bubbles in the foam grow, bi-axial extension orients the mesophase domains parallel to the cell walls, similar to the uni-axial extension (shear) during melt extrusion (or spinning) of mesophase pitch-based carbon fibers. As with carbon fiber production, the pitch foam is then stabilized by heating in air or oxygen for many hours to cross-link the structure, and "set" the pitch, so it does not melt during further heat treatment (16, 21). Stabilization can be a very time consuming and expensive process depending on the part size. The "stabilized" pitch foam is carbonized in an inert atmosphere to temperatures as high as 1100°C, producing a structural material suitable for composite reinforcement (22, 14, 16-20). As stated earlier, these foams are for structural composites, rather than thermal management materials (21-23).

A new, and less time consuming process for fabricating pitch-based graphitic foams without the traditional blowing and stabilization steps has been developed at Oak Ridge National Laboratory (ORNL) and is the focus of this research. More importantly, these new foams are extremely thermally conductive, compared to existing carbon foams. It is believed that these new foams will be less expensive and easier to fabricate than traditional foams since the time consuming oxidative stabilization step has been removed. Potentially, the process will lead to a significant reduction in the cost of carbon-based thermal management and structural materials (i.e. foam-reinforced composites and foam core sandwich structures).

The following discussions focus on foams produced from a synthetic mesophase pitch from Mitsubishi Gas Chemical Co. labeled ARA24. While others have been explored with success, the vast majority of the data has been focused on this pitch due to its availability.

2. Graphitic Foams

2.1 Microstructural Characterization

2.1.1 Pore Morphology

Figures 2 and 3 are scanning electron micrographs of the pore structure of the foams heat-treated at 1000°C and 2800°C. The foams exhibit a spherical structure with open, interconnected pores between most of the cells (P1 and P2). It is evident from the images that the graphitic structure is oriented parallel to the cell walls and highly aligned along the axis the ligaments (L). In fact, this feature is striking since it is clearly visible in foams with a final heat treatment of only 1000°C (Figure 2). Normally, in other graphitizable carbons, this texture is not clearly evident at these low temperatures. This highly aligned structure is significantly different from typical vitreous carbon foams: vitreous carbon foams are void of graphitic structure, have large openings and linear ligaments, and are mostly pentagonal dodecahedral in shape (Figure 1).

Moreover, it can be seen that in the junctions between ligaments, the graphitic structure is less aligned and possesses more folded texture. It is postulated that this arises from the lack of stresses at this location during forming. Therefore, the well ordered structure in these regions is primarily an artifact of the structure in precursor mesophase prior to heat treatment.

2.1.2 Optical Microstructure

Figure 4 displays optical micrographs of the foams under cross-polarized light with a quarterwave retarder. The micrographs reveal that the graphene layer planes are highly oriented parallel to the surface of the bubbles and along the axis of the ligaments, indicated by the

monochromatic regions (MC) in Figure 4. The lack of an oxidative stabilization allows the mesophase domains to grow very large during the processing, producing very few domain boundaries in the ligaments. The large optical domains that result are even evident in the pictures of the foams heat-treated to only 1000°C. The mesophase alignment is predominantly parallel to the surface of the bubbles, with a disruption of the alignment in the junctions. When the samples are graphitized, the alignment in the ligaments becomes more refined while the mesophase in the junctions becomes very folded. The multicolored regions in the images of the junctions between ligaments, (J in Figure 5), confirm that although these regions are graphitic, there is more fold-sharpening and random orientation of the crystals in these regions than that found in the ligaments. These regions will serve to limit the overall thermal conductivity (because of their increased thermal resistance compared to the ligaments), although the foam should still exhibit excellent thermal conductivity.

2.2 Thermal Conductivity

The thermal conductivity of the carbonized foams (Figure 6) was, as expected, very low (1-2 W/m·K) which is consistent with other porous carbon materials (14, 17, 19, 22, 23-27). The thermal conductivity of the graphitized foams, however, varied linearly with density from 50 to 150 W/m·K (Figure 7). This is remarkable for a material with such a low density, 0.27 to 0.57 g/cm^3.

The foam exhibits isotropic thermal conductivities comparable to the in-plane thermal conductivity of other thermal management materials and significantly higher than in the out-of-plane directions (Table 1). Although several of the other thermal management materials have higher in-plane thermal conductivities, their densities are much greater than that of the foam. Hence, the specific thermal conductivity (thermal conductivity divided by specific gravity) of the

foam (>300 W/m·K) is significantly greater than most of the available thermal management panels (in-plane and out-of-plane). In fact, the specific thermal conductivity is more than six times greater than copper and five times greater than aluminum, the preferred materials for heat sinks.

It is clear that for weight sensitive thermal management applications or applications where transient conditions often occur, the graphitic foam can be superior in thermal properties to other available materials. The advantage of isotropic thermal and mechanical properties combined with open celled structure should allow for novel designs that are more flexible and more efficient.

2.4 Mechanical Characterization

The mechanical properties of the foam and foam-based composites are presented in Table 2. The compressive strength of the foam was rather low (1-3 MPa) compared to carbon fibers. However, it compares well with some aluminum and Kevlar® honeycombs. When the samples were impregnated with an epoxy resin the compressive strength increased by an order of magnitude to 34.3 MPa, and the flexural strength, 19.5 MPa, approached that of commercial thermal management panels. Although similar compressive strengths, 31.6 MPa, and flexural strengths, 19.4 MPa, were achieved when the foam was densified with CVD carbon, the mode of failure was different, as shown in Figure 8. While both the raw graphitic foam and the resin- filled foam exhibited a high work of fracture, the CVD/foam material had a more brittle failure.

2.5 Foam-based Structures and Devices

Several foam core sandwich panels were fabricated by laminating the foam with aluminum and copper facesheets (0.5-mm thick). The isotropic thermal conductivity of these foam-core composites (see Figure 9) should provide thermal management characteristics comparable to existing materials but at a lighter weight, leading to more efficient thermal management materials

and, possibly, a new approach to thermal management. The foam is very versatile: it can be made in large samples, is easily machined, laminated with facesheets, or net shape formed. Also, successful densification with aluminum, carbon, epoxy, and thermoplastic resins has been accomplished, demonstrating the use of foam as the reinforcement in a composite structure where high thermal conductivity is required, but at a lower cost than traditional high conductivity carbon fibers.

To test this ability to transfer heat, the foam was machined into a finned heat sink resembling a standard aluminum heat sink from a Pentium 133 computer (see Figure 10). First, a 10W 2-in. x 2-in. heater was mounted beneath a 2-in. x 2-in. x 1/8-in. aluminum plate and placed at 90% output. The equilibrium temperature of the center of the aluminum plate was 170°F. The standard aluminum heat sink from the Pentium 133 computer was mounted on the aluminum plate and air was passed over it. The equilibrium temperature of the aluminum plate reached 99°F after 5 minutes. When the finned foam heat sink was mounted on the heater (after 170°F equilibrium was attained), the equilibrium temperature of the aluminum plate was 93°F (with the same air flow). Since the mass of the foam heat sink was significantly lower than the aluminum (8 g vs. 44 g), this was an important achievement. The foam is more efficient because the exposed surface area (due to the structure of the porosity) is larger than the aluminum heat sink. With this in mind, the fins were machined off the finned foam heat sink and the test repeated. Remarkably, the temperature of the aluminum plate equilibrated at 103°F. A significant achievement since the thin foam sink weighed only 4 grams (compared to 44 for the aluminum heat sink).

In a final test (see Figure 10), another finned foam heat sink was machined and installed on a Pentium 133 processor in an operational computer (the image analysis system used in this

research). As of the writing of this paper, it has been operating with the fan for 6 continuous months without problems.

4. Conclusions

The remarkable thermal properties of the foam described here (an isotropic bulk thermal conductivity as high as 150 W/m·K and a specific conductivity up to 6 times greater than that of copper) is potentially an enabling material for many technologies. These unique thermal properties, combined with the continuous graphitic open celled network throughout the foam (unlike carbon fiber reinforced composites), should lead to novel and interesting methods of thermal management.

Although the data and discussion presented in this paper illustrate the potential of this material to be an enabling technology for many applications, further work is needed. It is believed that through process optimization (the minimization of cracks and development of better orientation in the junctions) thermal conductivities of the foams could be improved. A full characterization of the kinetics of the foaming reaction should be undertaken in order to allow optimization of the process. Finally, the effects of bubble openings and heat treatment conditions on the mechanical and thermal properties, as well as heat transfer coefficients should be evaluated.

5. References

1. Shih, W. Development of Carbon-Carbon Composites for Electronic Thermal Management Applications. IDA Workshop, May 3–5, 1994.
2. Hexcel Product Data Sheet, 1997.
3. Gibson LJ, Ashby, MF. Cellular Solids: Structures & Properties, Pergamon Press, New York, 1988.

4. Adams, P.M.; Katzman, H.A.; Rellick, G.S.; Stupian, G.W. Characterization of high thermal conductivity carbon fibers and a self-reinforced graphite panel. Carbon, Vol: 36, Issue: 3, pp. 233-245, 1998.

5. Amoco Product Literature, 1997.

6. Steiner K, Banhard J, Baumister J, Weber M. Extended Abstracts, 4th International Conference on Composites Engineering, Kona, (Hawaii, USA), July 6-12, 1997: 943-944.

7. Glicksman LR, Torpey M. Proceedings of the Polyurethane World Congress, Aachen, Germany, 1987.

8. Glicksman LR, Marge AL, Moreno JD. Developments in Radiative Heat Transfer, ASME HTD – 1992;203.

9. Kuhn J, Int. J. Heat Mass Transfer 1992;35(7):1795-1801.

10. Glicksman, LR, Schuetz M, Sinofsky M. A Study of Radiative Foam Heat Transfer through Foam Insulation. Report prepared by Massachusetts Institute of Technology under subcontract No. 19X-09099C, 1988.

11. Ultramet Product Literature, 1998.

12. Doermann D, Sacadura JF. J. of Heat Transfer 1996;118:88-93.

13. Hagar JW Lake ML, Mat. Res. Soc. Symp. 1992;270:29-34.

14. Sandhu SS, Hagar JW. Mat. Res. Soc. Symp. 1992;270:35-40.

15. White JL, Sheaffer PM, Carbon 1989;27(5):697-707.

16. Bonzom A, Crepaux A, Moutard A. Process for preparing pitch foams and products so produced, The British Petroleum Company, U. S. Patent. 4276246, 1981.

17. Knippenberg, WF, Lersmacher B, Phillips Tech. Rev. 1976;36(4):93-103.

18. Aubert, JH, Mat. Res. Soc. Symp. 1990;207:117-127.

19. Cowlard FC, Lewis JC, J. of Mat. Sci. 1967;2:507-512.

20. Edie, DD. In: Figueiredo, J. L., et. al., editor. Carbon Fibers, Filaments, and Composites, Kluwer Academic Publishers, 1990:43-72.

21. Kearns K, The 21st Annual Conference on Ceramic, Metal, and Carbon Composites, Materials, and Structures, Cocoa Beach, Florida, 1997;835-847.

22. Hagar JW, Mat. Res. Soc. Symp. 1992;270:41-46.

23. Stiller A, Sral D, Plucinsk J, Zondlo J. The 22nd Annual Conference on Ceramic, Metal, and Carbon Composites, Materials, and Structures, January 26-31, Cocoa Beach, Florida, 1998.

24. Olhlorst CW, Vaughn WL, Ransone PO, Tsou H-T. Thermal Conductivity Database of Various Structural Carbon-Carbon Composite Materials. NASA Technical Memorandum 4787, November 1997.

25. ERG product literature, 1998.

26. Dinwiddie RB, Nelson GE, Weaver CE. Proceedings 23rd Int. Thermal Conductivity Conference, Technomic Pub. Co., Lancaster PA, 1996:466-477.

27. Wei GC, and Robbins JM. Ceramic Bulletin 1985;64(5):691-699.

Acknowledgements

The authors wish to thank Conoco Inc. for supplying the proprietary pitches for this research, Claudia Rawn of ORNL for performing the x-ray analysis of the foams and Marie Williams of ORNL for SEM and optical analysis of the foams.

Research sponsored by the U.S. Department of Energy, Assistant Secretary for Energy Efficiency and Renewable Energy, Office of Transportation Technologies, as part of the Advanced Automotive Materials Program, under Contract No. DE-AC05-96OR22464 with Lockheed Martin Energy Research Corporation.

Table 1. Thermal properties of carbon fiber composites and other thermal management materials.

Material	Specific Gravity	Thermal Conductivity		Specific Thermal Conductivity*	
		In-plane	Out-of-plane	In-plane	Out-of-plane
		[W/m·K]	[W/m·K]	[W/m·K]	[W/m·K]
Typical 2-D Carbon-Carbon [4]	1.88	250	20	132	10.6
EWC-300/Cyanate Ester [5]	1.72	109	1	63	0.6
Copper [5]	8.9	400	400	45	45
Aluminum 6061[5]	2.8	180	180	64	64
Aluminum Honeycomb [2]	0.19	--	~10	--	52
Aluminum Foam [6]	0.5	12	12	24	24

* Defined as thermal conductivity divided by specific gravity.

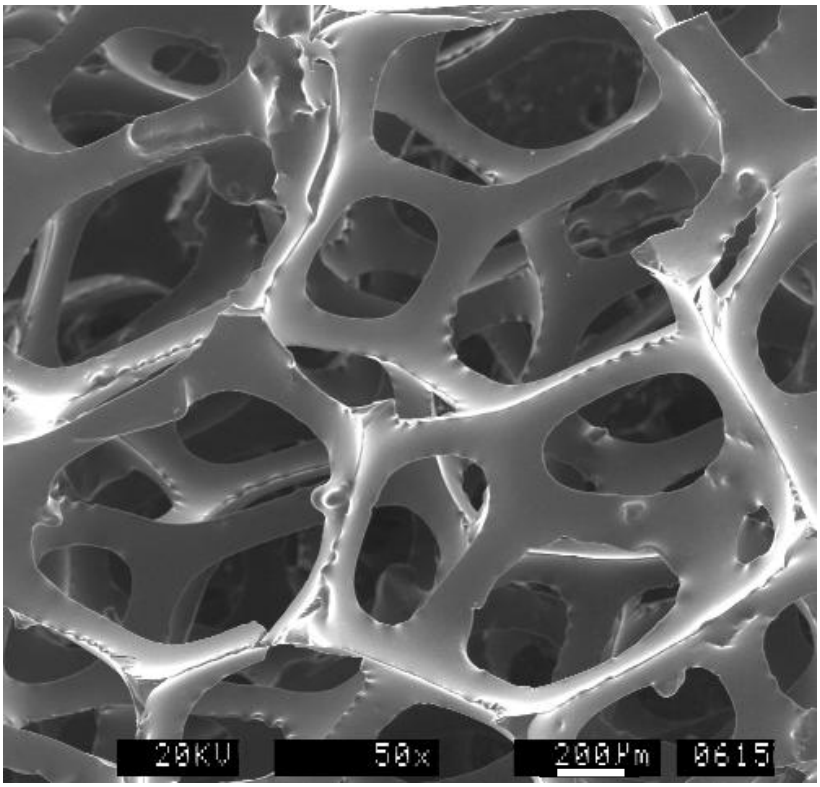

Figure 1. Typical reticulated glassy carbon foam produced by ERG Corporation.

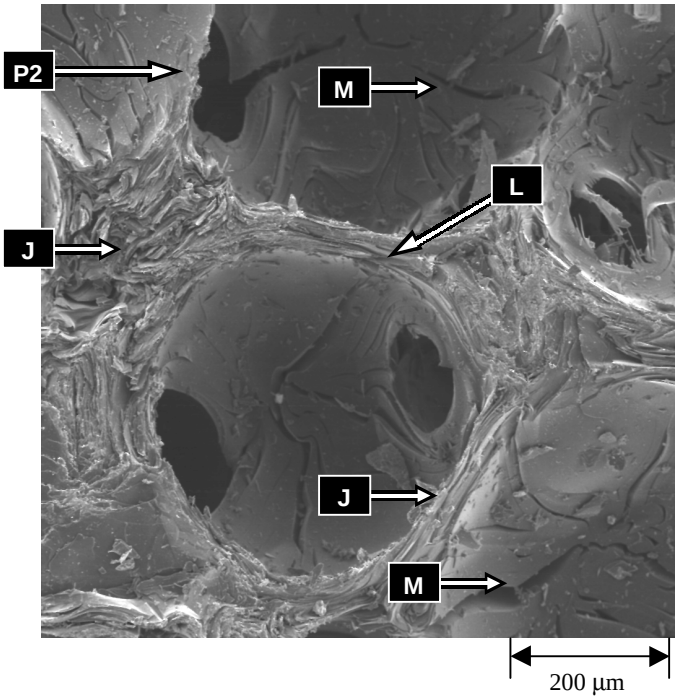

Figure 2. Structure of Mitsubishi ARA pitch-derived carbon foam carbonized at 1000°C.

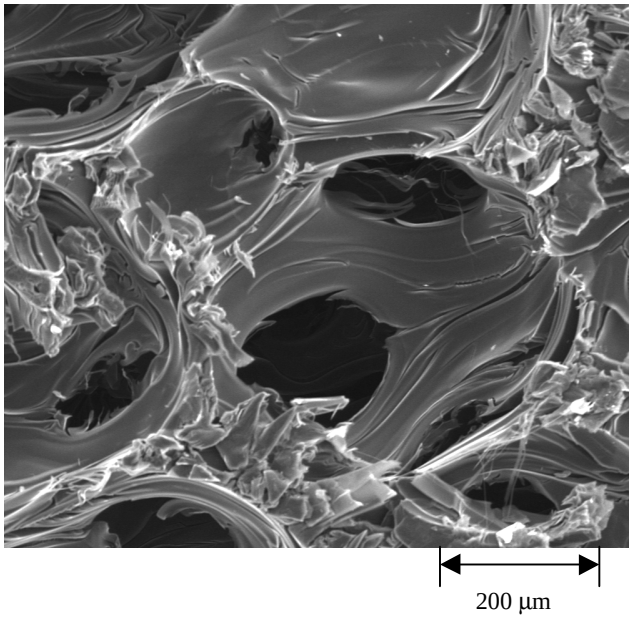

Figure 3. Structure of Mitsubishi ARA pitch-derived carbon foam graphitized at 2800°C.

.

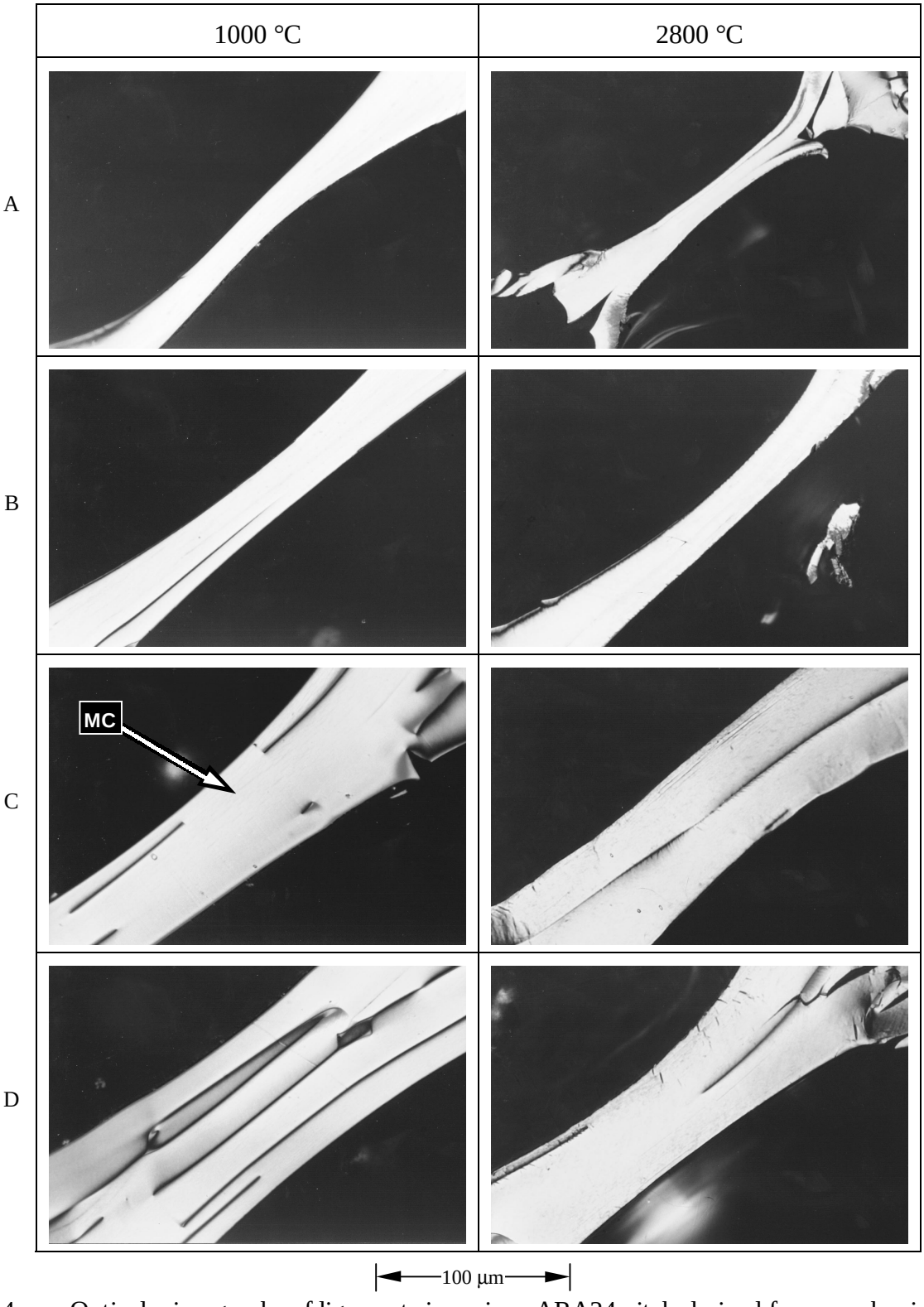

Figure 4. Optical micrographs of ligaments in various ARA24 pitch-derived foams carbonized at 1000°C and graphitized at 2800°C (Densities A < B < C < D).

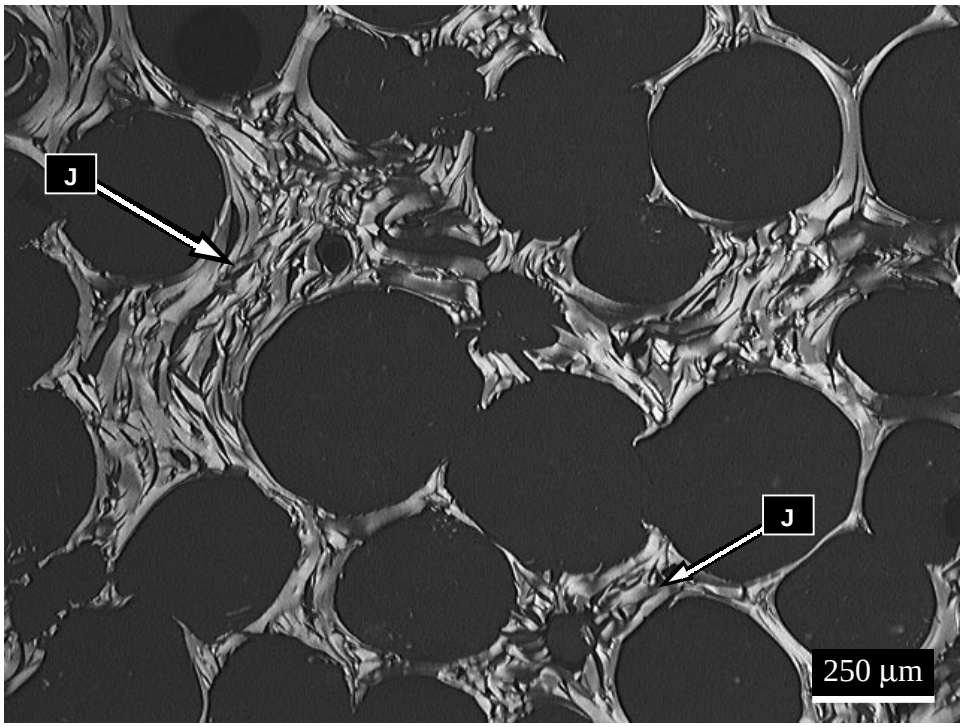

(a)

Figure 5. Comparison of flow texture in junctions and ligaments in ARA24 pitch-derived foams formed graphitized at 2800°C.

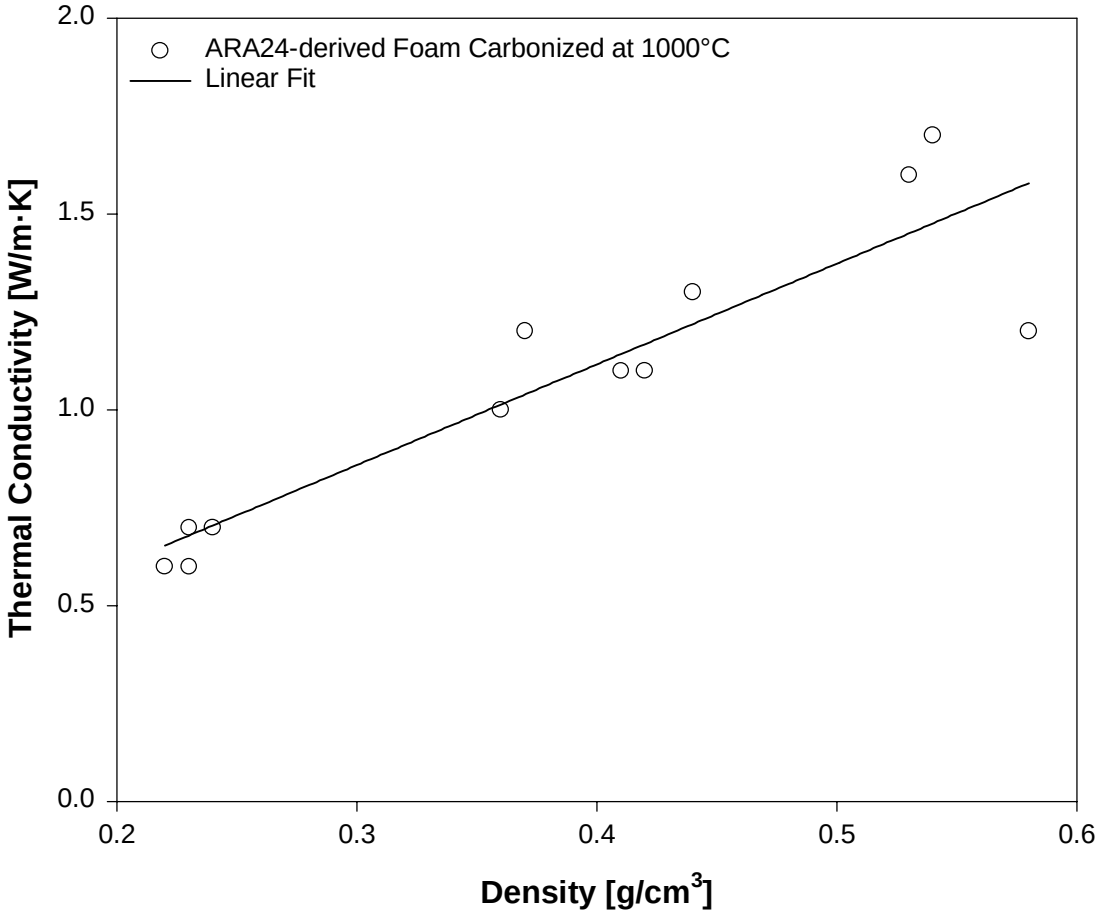

Figure 6. Thermal conductivity as a function of density for ARA Mesophase pitch-derived foams and Conoco-derived foams carbonized at 1000°C.

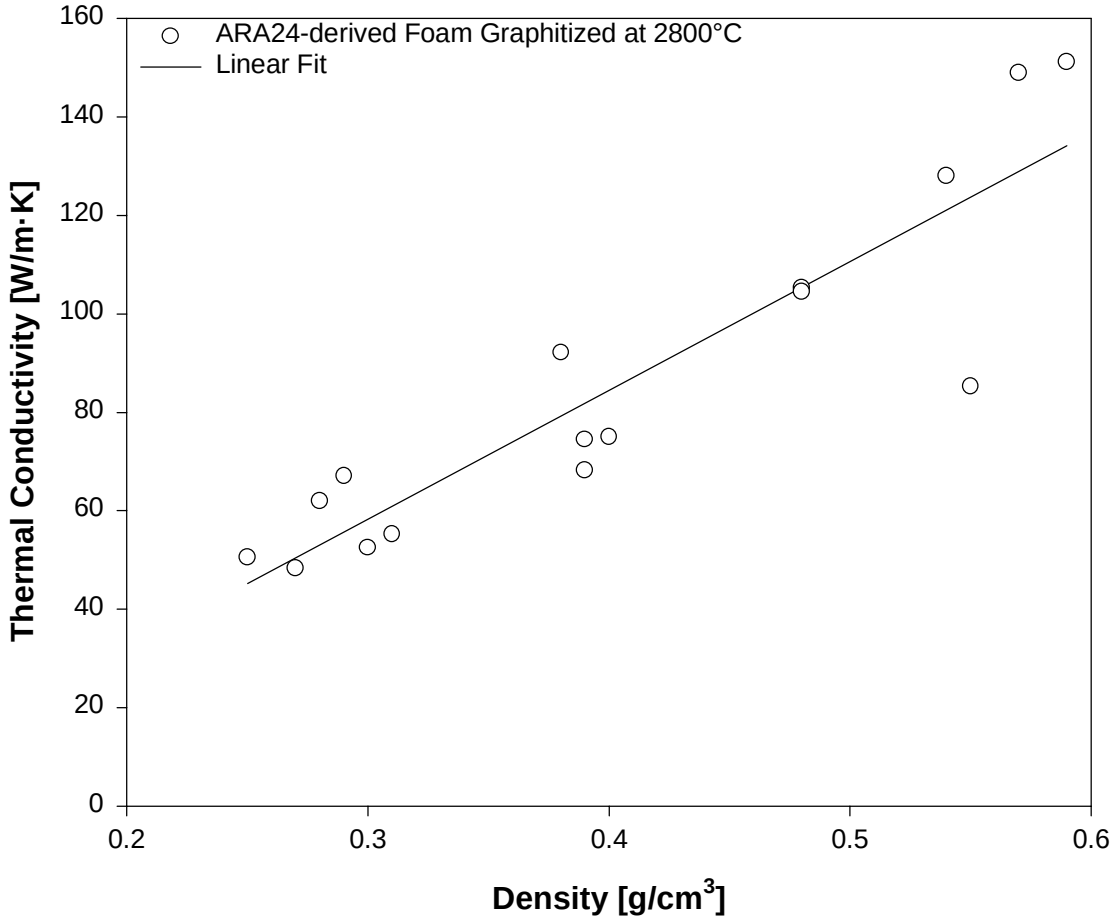

Figure 7. Thermal conductivity as a function of density for ARA Mesophase pitch-derived foams and Conoco-derived foams graphitized at 2800°C.

Table 2. Mechanical properties of foam and other thermal management panels.

Material	Specific Gravity	Flexural		Compressive	
		Strength	Modulus	Strength	Modulus
		MPa	**GPa**	**MPa**	**GPa**
ARA Foam	***0.54***			***1-3***	***.180***
ARA Foam /Epoxy	***1.26***	***19.5***	*--*	***34.3***	***.560***
ARA Foam /Carbon CVI	***1.3***	***19.4***	***2.3***	***31.6***	***.850***
EWC – 300X[5] K1100 (4K PW)/ERL 1939-3 resin	1.72	29.5†	13.1†	18.5	--
Aluminum Honeycomb[2] (CRIII 5052) ⅛ -in. cell size, 1 mil wall	0.07	--	--	3.7	1.030
Aluminum Honeycomb[2] (CRIII 5052) ⅛ -in. cell size, 3 mil wall	0.19	--	--	18.6	1.030
Kevlar Honeycomb[2] (HRH®-49) ¼" cell size	0.03	--	--	0.90	.172
Aluminum Foam[6]	0.5	--	--	~1.0	~1.0

†Tensile properties.

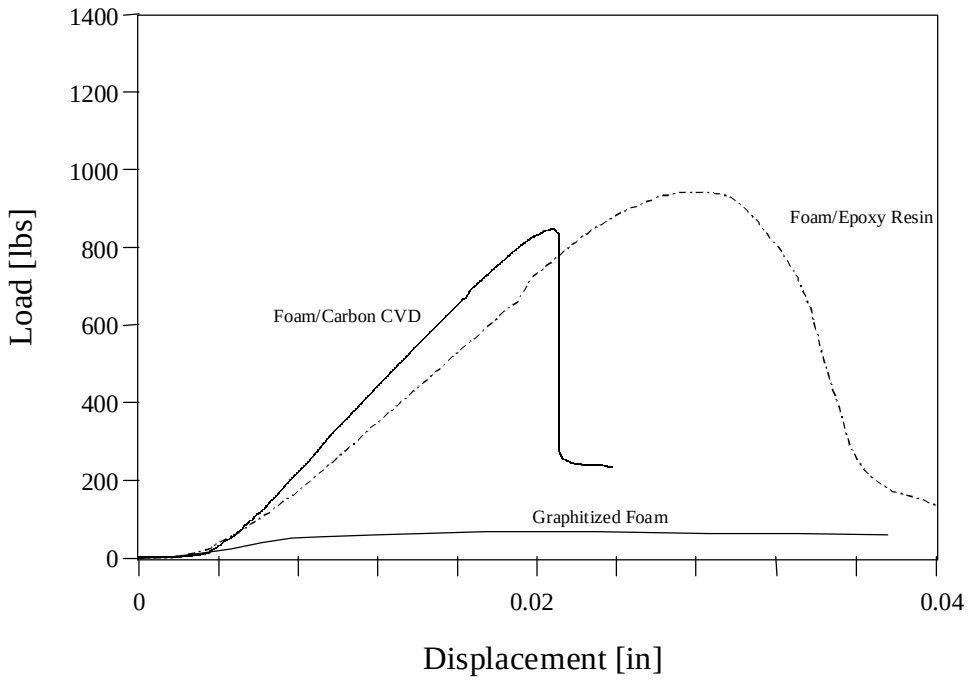

Figure 8. Compression tests of ARA 24 Pitch-derived carbon foam and foam derived composites.

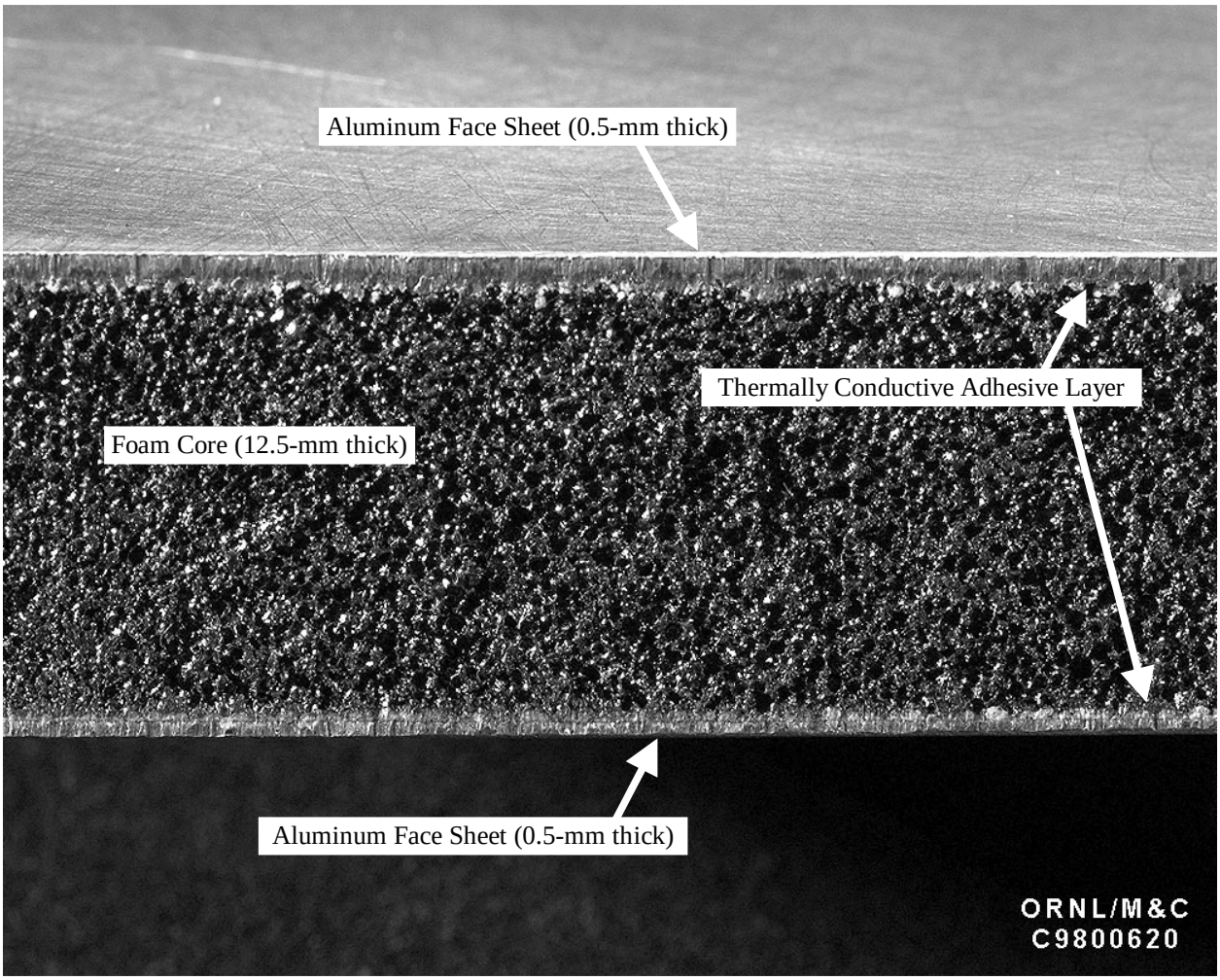

Figure 9. High thermal conductivity foam-core composite with aluminum face sheets.

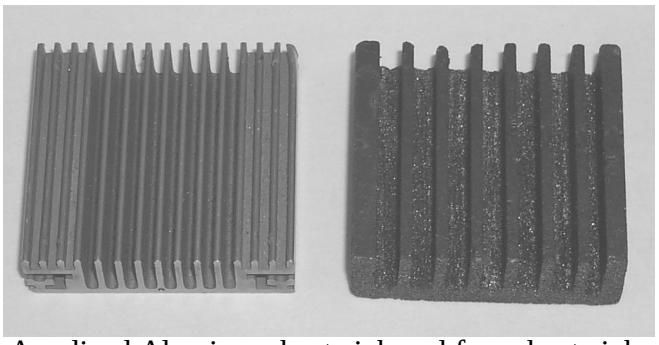

Anodized Aluminum heat sink and foam heat sink.

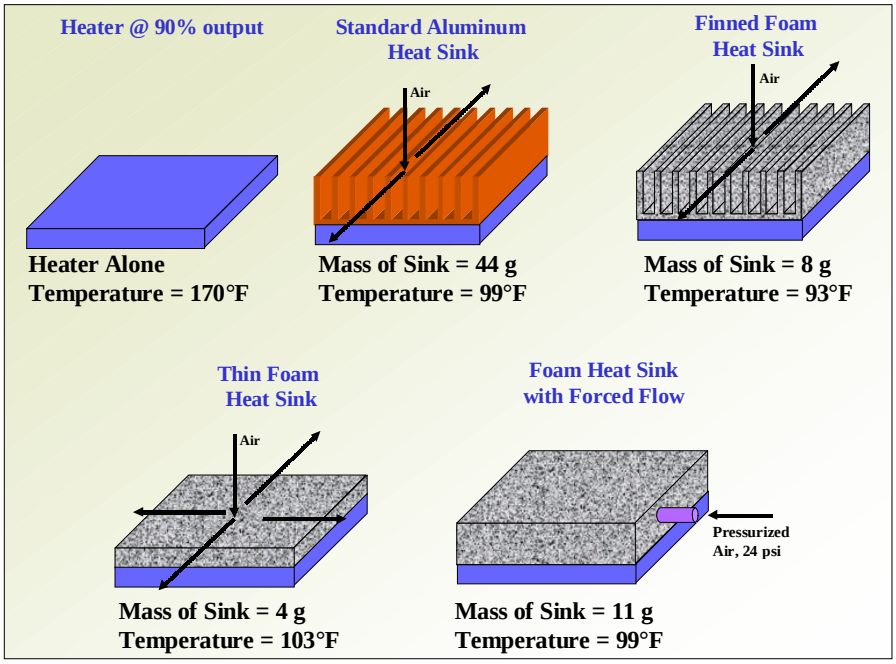

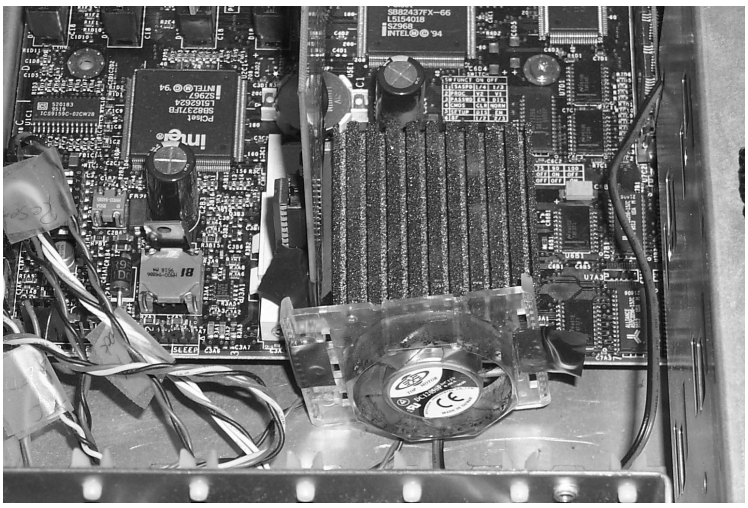

Foam heat sink in Pentium 133 computer

Figure 10. Computer chip heat sinks made from graphitic foam.